# Effect of thermal parameters and pH on obtaining copper ferrite via EDTA-Citrate complexation method

Larissa Nogueira e Silva[1], Maitê Medeiros de Santana e Silva [2],
Francisco Klebson Gomes dos Santos [1], Carlson Pereira de Souza [2],
André Luis Lopes Moriyama [2], Andarair Gomes dos Santos [1]

[1] Universidade Federal Rural do Semi-Árido, Departamento de Ciências Naturais, Matemática e Estatística, Av. Francisco Mota, Bairro Costa e Silva, 572, CEP: 59.625-900, RN, Mossoró, Brasil.
[2] Universidade Federal do Rio Grande do Norte, Departamento de Engenharia Química, Campus Universitário, Lagoa Nova, s/n, CEP: 59078-970, RN, Natal, Brasil.
e-mail: larissaengquimica@hotmail.com, andarair@ufersa.edu.br

## ABSTRACT

The synthesis of ceramic materials such as ferrite has been widely studied in recent years, due to their properties that make these materials have excellent applications in technology, as well as in photocatalytic processes and as catalysts. To obtain the copper ferrite phase the EDTA-Citrate complexation method was used, varying pH (5, 7 and 9), temperature (600, 800 and 1000 °C) and calcination time (2, 7 and 12 h). Composition, morphology and structural analyzes were performed by X-ray fluorescence spectroscopy, X-ray dispersive energy, scanning electron microscopy and X-ray diffraction, respectively. Crystalline phase of copper ferrite ($CuFe_2O_4$) with tetragonal structure and secondary phase of $Fe_2O_3$ and $CuO$ was verified by XRD analysis. Regarding the chemical composition analyzes, percentage deviations of the samples and the theoretical value for copper and iron were calculated. It was obtained minimum values of 0.16 - 0.08% (atomic%, EDS) and 16 - 8% (atomic%, XRF) in relation to copper and iron, respectively, for the sample obtained under pH 9, calcined at 600 °C for 12 h. The variation of the synthesis condition via EDTA-Citrate directly influenced the morphology of copper ferrite, presenting agglomerated particles, pore formation, irregular spheres, and even powder sintering.

keywords: thermal parameters, pH, copper ferrite, EDTA-Citrate, crystallinity and morphology.

## 1. INTRODUCTION

Spinel-type ferrite is a ceramic material that has been widely studied in recent years, for its magnetic properties, chemical and thermal stability, allowing these materials to have a variety of applications in technological areas such as energy integrated circuits, millimeter waves and magnets permanent [1] in addition to being used in photocatalytic processes [2], microwave radiation isolators [3], magnetic fluids [4], as well as catalysts [5]. Ferrite has crystalline structures and diverse compositions, with chemical formula $MFe_2O_4$, where M represents bivalent metallic cations, such as copper, cobalt, nickel, zinc, among others [6]. There are different techniques from which these materials can be synthesized, including sol-gel [2], co-precipitation [7], solvothermal [8], combustion [1], hydrothermal synthesis and EDTA-Citrate complexation [9]. This latter method has been widely used for the production of ceramic powders due to its numerous advantages, such as easy control of stoichiometry, high purity and crystallinity of the products, since the choice of a chemical process is very important to obtain good quality ferrite [10, 11].

Copper ferrite ($CuFe_2O_4$) may have a tetragonal or cubic structure, the first being more stable at low temperatures and the second at high temperatures [12]. Due to its low toxicity, thermal and chemical stability, this material can be used as a gas sensor, presenting high sensorial potential. YANG *et al.* [8] produced copper ferrite by the solvothermal method for gas sensor application, presenting excellent performance. They obtained a high and fast sensory response that exhibited a value of 20.1 to 250 °C, compared with the commercial gas detector responses that the maximum was 3.6 at that same temperature, besides presenting a characteristic of the nanospheres of copper ferrite. Studies show that this ferrite also has a recovery capacity when used as a catalyst, showing a loss of only 8% of the reaction yield after five subsequent cycles [13]. It can be used as a catalyst in organic reactions, such as phenol synthesis [14], Friedel-crafts acylation reactions [15] and alkoxylation of organic compounds [16]. SHETTY *et al.* [1] conducted a comparative study on copper, zinc and nickel ferrite, which were synthesized by the simple combustion method, and morphological

studies and photocatalytic studies were performed. The three ceramic materials presented efficiency as photocatalyst, but copper ferrite among the other synthesized materials presented higher photocatalytic potential in the decomposition of dyes with values of 94.5%, 82.8% and 65.3% for $CuFe_2O_4$, $NiFe_2O_4$ and $ZnFe_2O_4$, respectively.

The objective of this work is to obtain the copper ferrite synthesized by the EDTA-Citrate complexation method and to evaluate the influence of thermal parameters and pH on its chemical composition, structure and morphology.

## 2. MATERIALS AND METHODS

### 2.1 Synthesis of copper ferrite by EDTA-Citrate complexation method

The chemical reagents used in the synthesis of copper ferrite by the EDTA-Citrate complexation method were iron nitrate ($Fe(NO_3)_3.9H_2O$, Sigma-Aldrich), copper nitrate ($Cu(NO_3)_2.3H_2O$, Sigma-Aldrich), acid EDTA ($C_{10}H_{16}N_2O_8$, Synth). The three reagents were 99% pure, citric acid ($C_2H_4O_2$, Synth) 99.5% pure and ammonium hydroxide ($NH_4OH$, Impex) 28% pure in $NH_3OH$.

The EDTA-Citrate complexation method based on the methodology described by SANTOS *et al.* [10], SILVA *et al.* [11] and SILVA *et al.* [17] is shown in Figure 1 and briefly described below: initially, some amount of acidic EDTA was diluted in ammonium hydroxide at a ratio of 1 g:10 mL and kept under controlled stirring and heating (solution 1), then to solution 2 ($Fe(NO_3)_3.9H_2O$) and then solution 3 ($Cu(NO_3)_2.3H_2O$) was added to solution 1 and then solution 4. Subsequently citric acid was added (solution 4) and then the temperature was increased and controlled by about 80 °C until gel formation. The pH of solution 4 is corrected by the addition of $NH_3OH$ or with nitric acid solution (10 mol/L) when necessary. The molar ratio of acid EDTA, citric acid and metal ions to obtain ceramic powder was 1:1.5:1. Table 1 presents the experimental synthesis conditions. The pre calcination condition for all samples, regardless of pH, was the same: 230 °C, for 180 min with a heating rate of 5 °C/min.
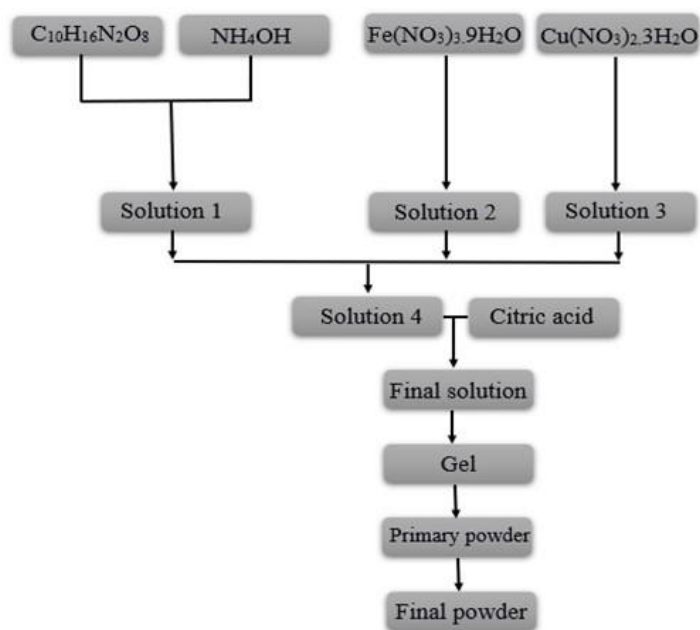


**Figure 1:** Proposed methodological route for $CuFe_2O_4$ synthesis based on the EDTA-Citrate complexation method.

**Table 1:** Experimental synthesis conditions for obtaining $CuFe_2O_4$ ceramic powders based on the EDTA-Citrate complexation method.

| Synthesis | Experimental conditions of synthesis | | | |
|---|---|---|---|---|
| | pH | Calcination (°C) | Rate (°C.min⁻¹) | Isotherm (h) |
| 1 | 5 | 600 | 5 | 2 |
| 2 | 9 | 600 | 5 | 2 |
| 3 | 5 | 1000 | 5 | 12 |
| 4 | 9 | 1000 | 5 | 12 |
| 5 | 5 | 600 | 5 | 12 |
| 6 | 9 | 600 | 5 | 12 |
| 7 | 5 | 1000 | 5 | 2 |
| 8 | 9 | 1000 | 5 | 2 |
| 9 | 7 | 800 | 5 | 7 |
| 10 | 7 | 800 | 5 | 7 |
| 11 | 7 | 800 | 5 | 7 |

### 2.2 Structural and morphological characterizations

The samples were characterized by X-ray Diffraction (XRD) in order to identify the crystalline phases. The measurements were obtained with an X-ray diffractometer (Shimadzu DRX-7000), using Cu-Kα radiation, with 40 kV voltage and 30 mA current. The diffractograms were obtained in the 2θ range ranging from 10 to 80 degrees in 5 °C/min steps. To identify the crystalline phase (s), the X´Pert High Score version 4.8 software was used.

The morphology of the samples was evaluated by field emission scanning electron microscopy (SEM) (MEV-FEG) (Carl Zeiss, Auriga model) coupled with dispersive energy spectrometer (EDS), which was used for Chemical composition analysis, which was also obtained by X-ray Fluorescence Spectroscopy, using an EDX-7000 Shimadzu detector spectrometer. The enlargements were performed on a scale of 1 micrometer (1 μm) and / or 200 nanometers (200 nm).

### 3. RESULTS

### 3.1 X-ray diffraction (XRD) of EDTA-Citrate copper ferrite

Figure 2 shows the diffractograms of $CuFe_2O_4$ samples synthesized via EDTA-Citrate complexation method, as shown in Table 1.

Figure 2 (A) shows the diffractograms of the samples synthesized in an acid medium (pH 5) with different temperature conditions and calcination time according to Table 1. Analyzing the samples obtained at 600 °C with different isotherm times, it was found that the sample is composed of iron oxide ($Fe_2O_3$). And, the increase in the calcination time favors the formation of the desired phase. In general, the temperature of 600 °C is not sufficient to obtain pure copper ferrite by EDTA-Citrate complexation method independent of the isotherm time since the material is partially amorphous together with a mixture of oxides for the synthesis condition in pH 5. However, maintaining pH 5 and thermally treating at 1000 °C for 2 h and 12 h, in both isotherms more well-defined peaks can be observed, and the presence of single-phase $CuFe_2O_4$ can be identified, according to the crystallographic plans presented in the diffractogram.

Samples synthesized at pH 7 with calcination conditions of 800 °C for 7 h are shown in Figure 2 (B). This experimental condition synthesized in triplicate presents better defined peaks, characteristic of crystalline solids, indexed as a spinel of copper ferrite. Finally, the diffractograms for samples synthesized with pH 9 are shown in Figure 2 (C). In a basic reaction medium and at 600 °C, a noticeable difference is noticed in the formation of the desired phase depending on the calcination time, where the heat-treated sample for 2 h presents a mixture of oxides while the increase in the treatment time for 12 h results in a more crystalline material that presents only copper oxide as impurity. However, when calcined at 1000 °C and basic medium, they are monophasic and crystalline regardless of the calcination time.
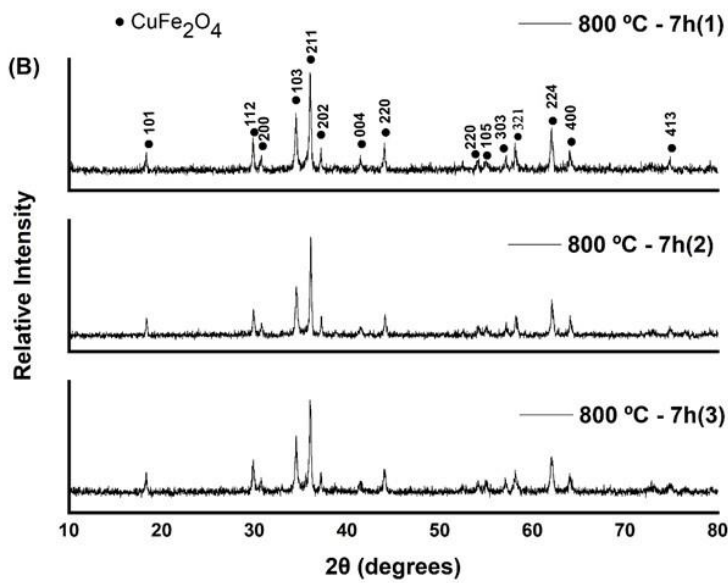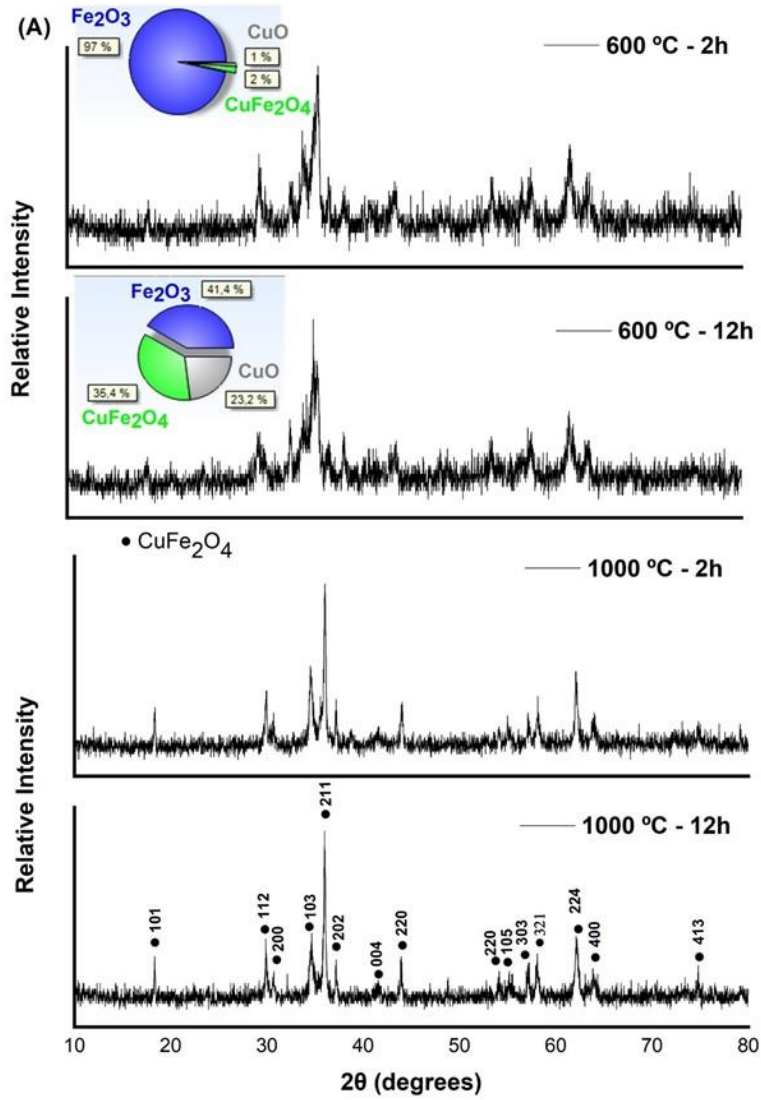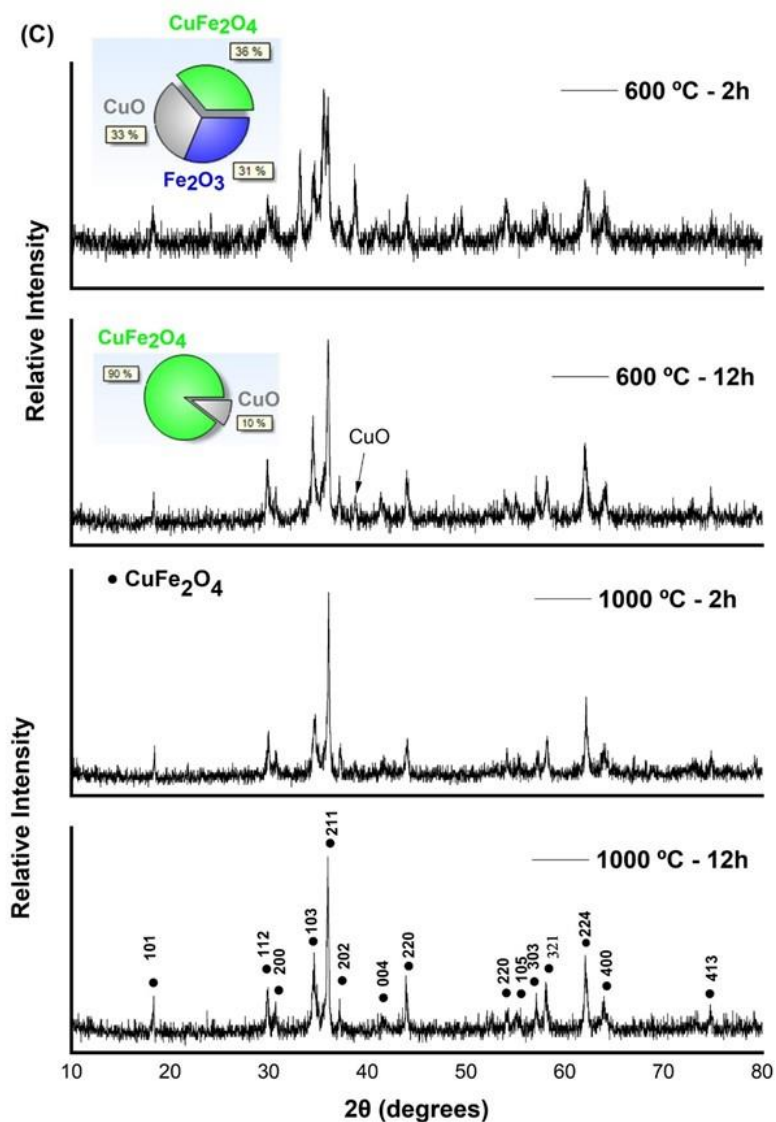
**Figure 2:** Copper Ferrite Diffractograms (A) pH 5, (B) pH 7 e (C) pH 9.

The XRD standards used to identify the samples obtained (Figure 2) are the tetragonal copper ferrite spinel (I41 / amd (141), ICSD N°: 016666), rhombohedral iron oxide (R-3c (167), ICSD N°: 022505 and monoclinic copper oxide (C2 / c (15), ICSD N°: 067850). There were no additional peaks related to the secondary phase in the diffraction patterns in samples pH 5 (1000 °C - 2 and 12 h) pH 7 (800 °C - 7 h) and pH 9 (1000 °C - 2 and 12 h), ensuring phase purity within the limit of XRD detection.

The results presented for the materials obtained in different experimental conditions showed that regardless of the pH of the synthesis it was not possible to obtain the desired pure phase when the organometallic complex was calcined at a temperature of 600 °C even when the isotherm time was increased by 2 for 12 h of time, however, when the calcination temperature was 1000 °C, the formation of copper ferrite free of impurities is verified, which leads us to believe that the temperature variable has greater influence within the process of formation of the desired material when synthesized by the EDTA-Citrate complexation method. With the increase mainly in temperature and followed by the reaction time, there is an increase in the internal energy and entropy of the system. To minimize the disorder caused, the crystals coalesce with each other due to the greater energy provided by the system, resulting in a crystalline material with a stable phase [9].

Although pH is a very important variable in complexation reactions, it is observed that in this case, it did not cause a significant change in the structure or phase formation for temperatures of 800 - 1000 °C for the studied calcination times. When analyzing the heat treatment condition at 600 °C at pH 5 and 9, the desired non-formation is observed, with the exception of the sample obtained in basic medium at 600 °C with 12 h of isotherm where the formation of ferrite is observed copper and a small amount of copper oxide.

NIKOLIĆ *et al.* [7] synthesized copper ferrites by the coprecipitation method in the same temperature

range (300 °C to 1100 °C) and observed the presence of iron oxide ($Fe_2O_3$) in all calcination temperatures, in addition to the formation of the copper oxide (CuO) at a temperature of 500 °C. SHETTY *et al.* [1] also synthesized copper ferrites using the simple combustion method at 500 °C, verified the presence of two secondary phases, $Fe_2O_3$ and CuO. From there, it can be seen that the method and the synthesis conditions are fundamental to obtain crystalline powders with an impurity-free phase. The methodology used for the production of copper ferrites calcined at 800 - 1000 °C, regardless of the pH of the synthesis, proved to be quite efficient with regard to obtaining single-phase powders since the literature shows that $CuFe_2O_4$ has already been produced by different methods in this same temperature range to no avail.

### 3.2 Chemical Composition Analysis by X-ray Fluorescence Spectroscopy (XRF)

By X-ray Fluorescence Spectroscopy analysis, the chemical composition of the synthesized samples was studied. Table 2 presents the atomic percentage values (at. %) of copper and iron for the samples analyzed, in addition to the deviation from the theoretical value.

**Table 2:** Chemical composition of $CuFe_2O_4$ analyzed by XRF.

| Samples | % Cu | Error (%) | % Fe | Error (%) |
|---|---|---|---|---|
| pH 5 (600 °C / 12h) | 39.86 | 19.59 | 60.14 | 9.80 |
| pH 5 (1000 °C / 2h) | 42.53 | 27.59 | 57.47 | 13.80 |
| 1- pH 7 (800 °C / 7h) | 44.39 | 33.16 | 55.62 | 16.58 |
| 2- pH 7 (800 °C / 7h) | 43.51 | 30.52 | 56.49 | 15.26 |
| 3- pH 7 (800 °C / 7h) | 44.46 | 33.39 | 55.54 | 16.69 |
| pH 9 (600 °C / 12h) | 38.66 | 15.99 | 61.34 | 7.99 |
| pH 9 (1000 °C / 2h) | 44.08 | 32.24 | 55.92 | 16.12 |

The theoretical atomic percentage of copper and iron are 33.33 and 66.67%, respectively, analyzing only these two atoms in the molecule. There are relatively high deviations between the atomic percentages obtained by XRF and the theoretical value, with minimum values 16 and 8% and maximum values 33 and 17% for copper and iron, respectively. The sample obtained under pH 9 conditions, calcined at 600 °C for 12 h, showed the smallest deviation among all synthesized samples. Deviations between the theoretical and experimental percentage may be related to the formation of secondary phases [18] identified in diffractograms and also to losses during material processing. Another point to be made is that the reagents used are hygroscopic in nature and during the weighing process, despite careful handling of the reagents, they absorb water quickly and this error may be embedded in the theoretical stoichiometric calculation to obtain of copper ferrite.

### 3.3 Morphological analysis by scanning electron microscopy (SEM)

The following Figures present the results of scanning electron microscopy (SEM) analysis of $CuFe_2O_4$ samples obtained via EDTA-Citrate complexation method under different conditions as shown in Table 1. Figure 3 (A) and Figure 3 (B) show magnification of 10000x and 20000x, respectively. The morphology of the sample with synthesis conditions: pH 5, calcined at 600 °C for 2 h and those of the pH 5 sample (magnified on the same scale) calcined at 600 °C for 12 h (Figure 4), are non-uniform and present pores. These results are similar to those of SHETTY *et al.* [1] that calcined the samples at 500 °C and obtained by microscopic analysis, structures with pores.
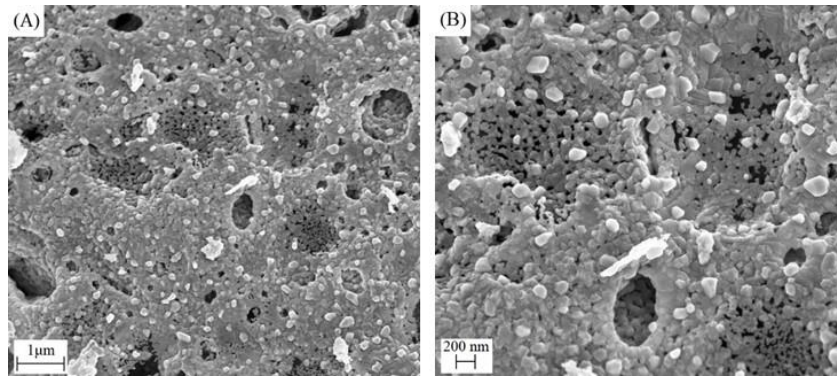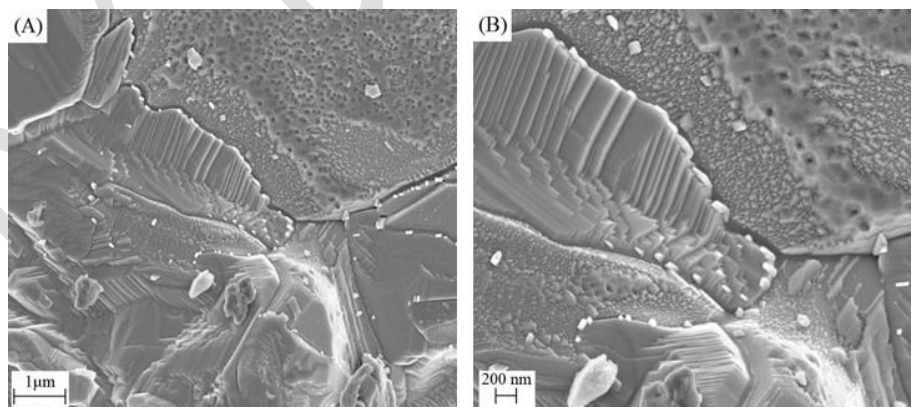
**Figure 3:** Scanning electron microscopy of CuFe$_2$O$_4$ sample obtained at pH 5 (600 °C / 2 h) conditions. (A) 1 μm and (B) 200 nm.
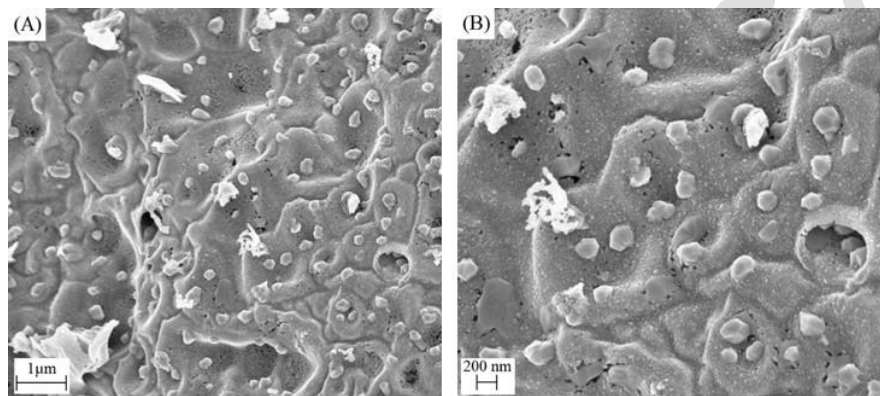


**Figure 4:** Scanning electron microscopy of CuFe$_2$O$_4$ sample obtained at pH 5 (600 °C / 12 h) conditions. (A) 1 μm and (B) 200 nm.

Figure 5 represents a pH 5 sample calcined at 1000 °C for 2 h. Being (A) and (B) with magnifications of 10000x and 20000x, respectively. When calcined at 1000 °C, the sample exhibits characteristics of a sintering process.



**Figure 5:** Scanning electron microscopy of CuFe$_2$O$_4$ sample obtained at pH 5 (1000 °C / 2 h) conditions. (A) 1 μm and (B) 200 nm.

Figures 6, 7 and 8 represent CuFe$_2$O$_4$ samples at pH 7 conditions, calcined at 800 °C for 7 h. Figures (A) have magnification of 10000x and figures (B) of 20000x. It is observed in the other irregular and agglomerated spherical particles, with similar shapes to those obtained by MANIKANDAN *et al.* [19].
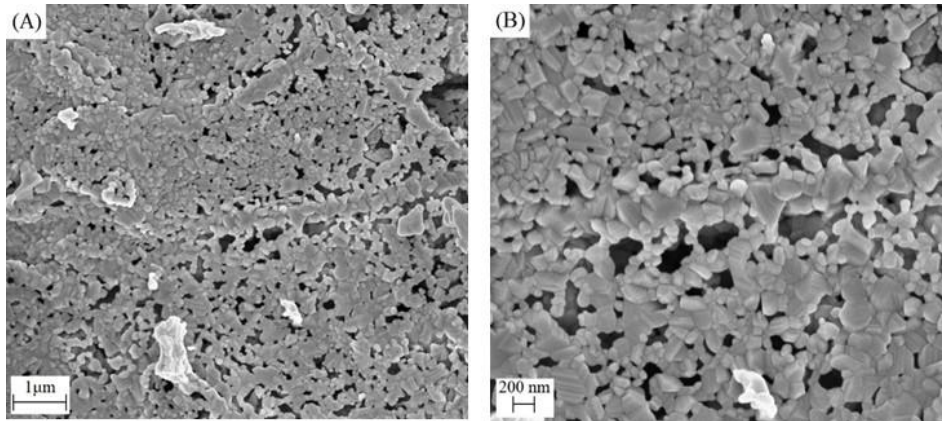
**Figure 6:** Scanning electron microscopy of CuFe$_2$O$_4$ sample obtained at pH 7 sample (1) conditions (800 °C / 7 h). (A) 1 μm and (B) 200 nm.
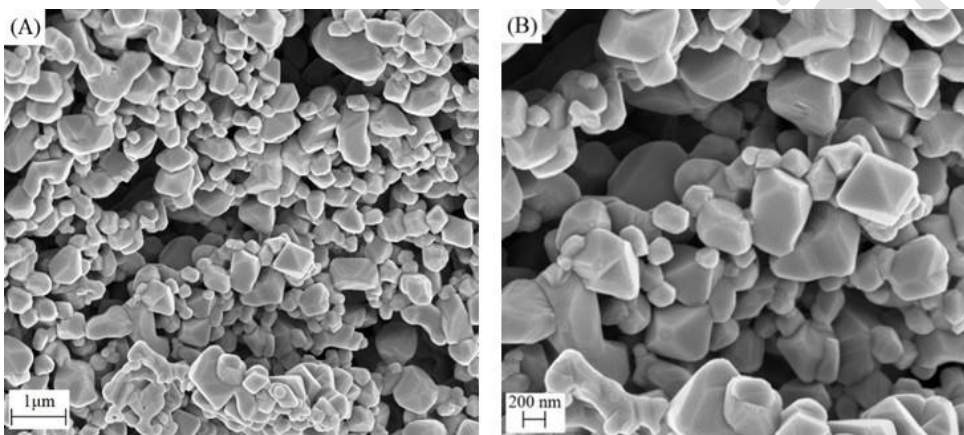


**Figure 7:** Scanning electron microscopy of CuFe$_2$O$_4$ sample obtained at pH 7 sample (2) conditions (800 °C / 7 h). (A) 1 μm and (B) 200 nm.
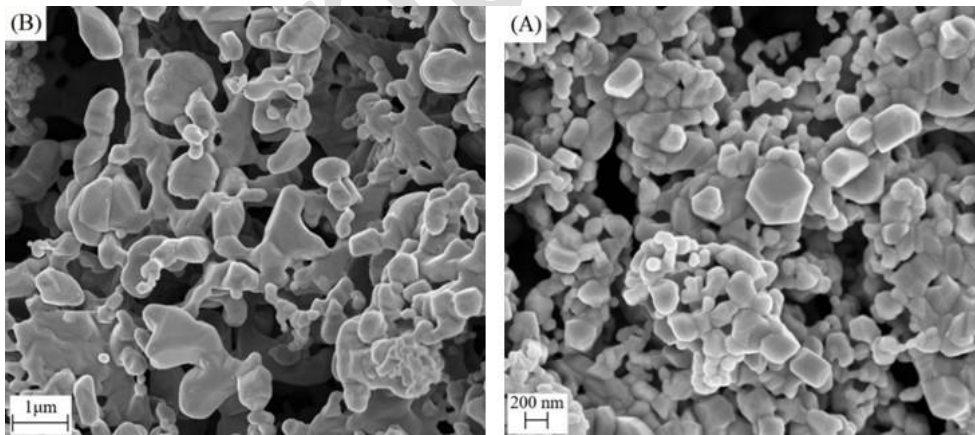


**Figure 8:** Scanning electron microscopy of CuFe$_2$O$_4$ sample obtained at pH 7 sample (3) conditions (800 °C / 7 h). (A) 1 μm and (B) 200 nm.

Figure 9, where (A) has magnification of 10000x and (B) of 20000x, obtained with conditions of pH 9 at 600 °C for 12 h, particle agglomerates, as well as the presence of small pores. While Figures 10 are samples of pH 9, the calcination conditions being: (A) 600 °C for 2 h, (B) 1000 °C for 2 h and (C) 1000 °C for 12 h. In these samples, particles with different shapes and non-uniform sizes are observed.
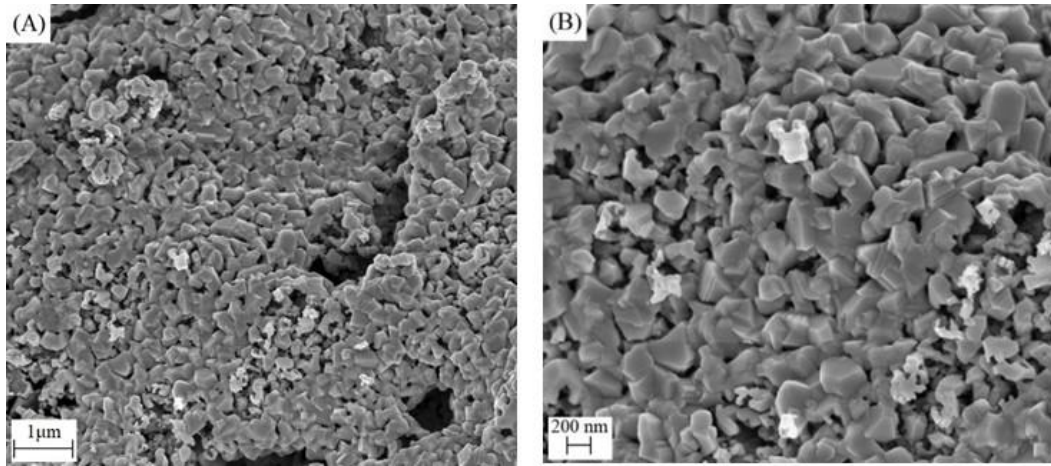
**Figure 9:** Scanning electron microscopy of CuFe$_2$O$_4$ sample obtained at pH 9 (600 °C / 12 h) conditions. (A) 1 μm and (B) 200 nm.
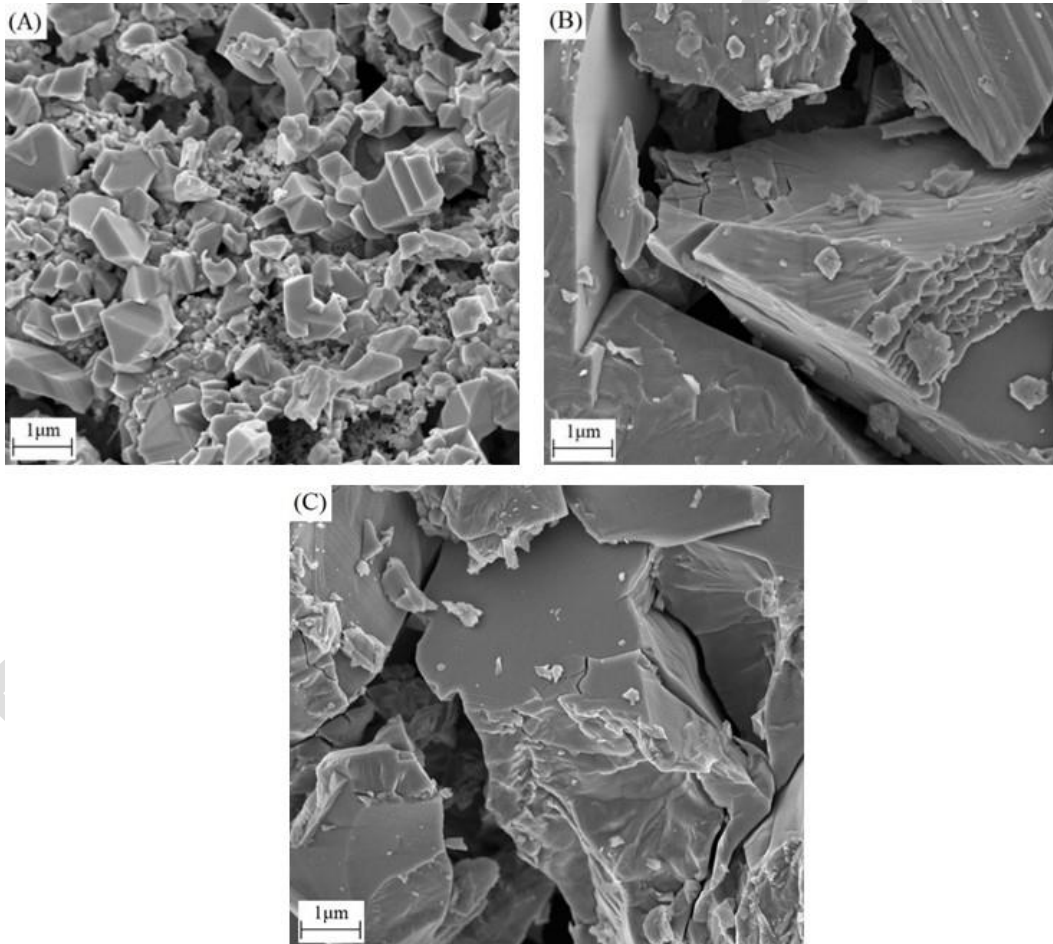


**Figure 10:** Scanning electron microscopy of CuFe$_2$O$_4$ sample obtained at pH 9 conditions - 1 μm (A) 600 °C / 2 h, (B) 1000 °C / 2 h and (C) 1000 °C / 12 h.

The different synthesis conditions influenced the morphology of the samples, presenting non-uniform shapes and sizes with inhomogeneous particle agglomerations.

Table 3 presents the atomic percentage values of copper and iron for the samples analyzed by X-ray dispersive energy (EDS), in addition to the deviation from the theoretical value.

**Table 3:** Chemical composition of $CuFe_2O_4$ analyzed by EDS.

| Samples | | % Cu | Error (%) | % Fe | Error (%) |
|---|---|---|---|---|---|
| Multiphase | pH 5 (600 °C / 2h) | 33.17 | 0.49 | 66.83 | 0.25 |
| Multiphase | pH 5 (600 °C / 12h) | 34.93 | 4.79 | 65.07 | 2.39 |
| Single phase | pH 5 (1000 °C / 2h) | 30.71 | 7.87 | 69.29 | 3.94 |
| Multiphase | pH 5 (1000 °C / 12h) | 29.79 | 10.63 | 70.21 | 5.32 |
| Single phase | 1- pH 7 (800 °C / 7h) | 33.91 | 0.37 | 66.09 | 0.87 |
| Single phase | 2- pH 7 (800 °C / 7h) | 33.18 | 0.46 | 66.82 | 0.25 |
| Single phase | 3- pH 7 (800 °C / 7h) | 34.12 | 2.36 | 65.88 | 1.18 |
| Multiphase | pH 9 (600 °C / 2h) | 31.52 | 5.44 | 68.48 | 2.63 |
| Multiphase | pH 9 (600 °C / 12h) | 33.28 | 0.16 | 66.72 | 0.08 |
| Single phase | pH 9 (1000 °C / 2h) | 32.22 | 3.34 | 67.78 | 1.67 |
| Multiphase | pH 9 (1000 °C / 12h) | 26.35 | 20.95 | 73.65 | 10.48 |

The deviations between the atomic percentages of the synthesized samples and the theoretical value were calculated, obtaining minimum values 0.16 and 0.08% and maximum values 20.95 and 10.48% for copper and iron, respectively. Such minimum deviation values were found in the sample obtained under pH 9 conditions, calcined at 600 °C for 12 h. The values obtained in the analysis can be considered reliable within the margin of error and the equipment itself, in the case of a semi-quantitative analysis.

## 4. CONCLUSIONS

Single-phase $CuFe_2O_4$ was obtained via EDTA-Citrate complexation method regardless of the pH of the medium (pH 5, 7 or 9), however the heat treatment adopted directly influences the purity of the phase. Among the experimental conditions studied, pure copper ferrite was obtained when synthesized in an acidic and basic medium at 1000 °C for 2 h and neutral pH at 800 °C for 7 h. The different synthesis conditions directly influenced the morphology of copper ferrite obtained by EDTA-Citrate method. Variations in particle agglomeration, pore formation and irregular sphere shapes were observed, as well as sintering the powder.

## 5. ACKNOWLEDGMENT

## 6. BIBLIOGRAPHY

[1] SHETTY, K., RENUKA, L., NAGASWARUPA, H.P., *et al.,* "Comparative study on $CuFe_2O_4$, $ZnFe_2O_4$ and $NiFe_2O_4$: Morphology, Impedance and Photocatalytic studies", *Materials Today*, pp. 11806-11815, 2017.

[2] SHARMA, R., SINGHAL, S., "Photodegradation of textile dye using magnetically recyclable heterogeneous spinel ferrites", *Journal of Chemical Technology & Biotechnology*, v. 90, pp. 955-962, 2015.

[3] KUANR, B.K., VEERAKUMAR, V., MARSON, R., *et al.* "Nonreciprocal microwave devices based on magnetic nanowires", v. 94, pp. 202505, 2009.

[4] SUJATHA, C., REDDY, K.V., BABU, K.S., *et al.* "Effects of heat treatment conditions on the structural and magnetic properties of MgCuZn nano ferrite", *Ceramics international*, v. 38, pp. 5815-5820, 2012.

[5] BALDISSERA, M.R., SILVA, M.R.A., SILVEIRA C.A., *et al.* "Síntese e caracterização de ferritas de Zn e Mn provenientes de pilhas inutilizadas", *Cerâmica*, v. 60, pp. 52-56, 2014.

[6] LEAL, E., DANTAS, J., OLIVEIRA, P.L., *et al.* "Avaliação da formação do híbrido $NiFe_2O_4@SiO_2$ e sua performance na immobilization of GOx", *Revista matéria,* v. 23, 2018.

[7] NIKOLIĆ, V.N., VASIĆ, M., MILIĆ, M.M., "Observation of low- and high-temperature $CuFe_2O_4$ phase at 1100 °C: The influence of $Fe^{3+}$ ions on $CuFe_2O_4$ structural transformation", v. 44, pp. 21145-21152, 2018.

[8] YANG, X., ZHANG S., YU, O., *et al.* "Solvothermal synthesis of porous $CuFe_2O_4$ nanospheres for high performance acetone sensor", *Sensors and Actuators B: Chemical*, v. 270, pp. 538-544, 2018.

[9] DE MEDEIROS, I.A.F., MORIYAMA, A.L.L., SOUZA, C.P., "Effect of synthesis parameters on the size of cobalt ferrite crystallite", *Ceramics International,* v. 43, pp. 3962-3969, 2017.

[10] SANTOS, A.G., COSTA, I.K.F., SANTOS, F.K.G., *et al.* "Efeito do método de complexação combinando EDTA - citrato e coprecipitação em meio oxalato na síntese da $SrCo_{0,8}Fe_{0,2}O_{3-\delta}$, *"HOLOS"*, v. 3, pp. 30-43, 2015.

[11] SILVA, M.M.S., SENA, M.S., LOPES-MORIYAMA, A.L., *et al.* "Experimental planning of the synthesis of strontium molybdate by EDTA-citrate and its structural influence, morphology and optical bandgap", *Ceramics International*, v. 44, pp. 16606-16614, 2018.

[12] PHABHU, D., NARAYANASAMY, A., SHINODA, K., *et al.* "Grain size effect on the phase tranformation temperature of nanostructred $CuFe_2O_4$", *Journal of Appied physics*, v. 112, pp. 39-44, 1994.

[13] CASAGRANDE, D.S., COSTA, W.V., HECHENLEITNER, A.A.W., *et al.* "Síntese e caracterização de nanopartículas de ferritas do tipo $Zn_xCu_{1-x}Fe_2O_4$ e a sua aplicação como catalisador em acetilação em óleos vegetais", In: *Congresso brasileiro de engenharia e ciência dos materiais*, pp. 1964-1975, Natal, 2016.

[14] YANG, D., AN, B., WEI, W., *et al.* "A novel sustainable strategy for the synthesis of phenols by magnetic $CuFe_2O_4$-catalyzed oxidative hydroxylation of arylboronic acids under mild conditions in water", *Tetrahedron*, v. 70, pp. 3630–3634, 2014.

[15] PARELLA, R., NAVEEN, KUMAR, A., *et al.* "Catalytic Friedel–Crafts acylation: magnetic nanopowder $CuFe_2O_4$ as an efficient and magnetically separable catalyst", *Tetrahedron Letters*, v. 54, pp. 1738-1742, 2013.

[16] YANG, S., XIE, W., ZHOU, H., *et al.* "Alkoxylation reactions of aryl halides catalyzed by magnetic copper ferrite", *Elsevier*, v. 69, pp. 3415-3418, 2013.

[17] SILVA, A.R., QUIXADÁ, G.F., SANTOS, P.E.C., *et al.* "Avaliação da perovsquita $BaCeO_3$ como catalisador na conversão de óleo de soja em biodiesel via rota etílica", In: Andrade, D. E. (org), *Petróleo e Outros Combustíveis,* 1 ed., capítulo 9, Belo Horizonte, Poisson, 2019.

[18] OH, W.D., DONG, Z., HU, Z.T., *et al.* "A novel quasi-cubic $CuFe_2O_4$–$Fe_2O_3$ catalyst prepared at low temperature for enhanced oxidation of bisphenol A via peroxymonosulfate activation", *Journal of Materials Chemistry A*, v. 44, pp. 22208-22217, 2015.

[19] MANIKANDAN, V., VANITHA, A., KUMAR, E.R., *et al.* "Effect of in substitution on structural, dielectric and magnetic properties of $CuFe_2O_4$ nanoparticles", *Journal of Magnetism and Magnetic Materials*, v. 423, pp. 477-483, 2017.

**ORCID**

Larissa Nogueira e Silva                    https://orcid.org/0000-0001-9462-4663
Maitê Medeiros de Santana e Silva           https://orcid.org/0000-0002-5368-8502
Francisco Klebson Gomes dos Santos          https://orcid.org/0000-0003-4542-6382
Carlson Pereira de Souza                    https://orcid.org/0000-0003-0736-0394
André Luis Lopes Moriyama                   https://orcid.org/0000-0001-7611-2074
Andarair Gomes dos Santos                   https://orcid.org/0000-0002-8565-2192